UNIVERSITY of CALIFORNIA
SANTA CRUZ

CHARACTERIZATION OF IRRADIATED SILICON SENSORS: WITH TIME OVER THRESHOLD, COUNT RATE, AND CLUSTER SIZE

A thesis submitted in partial satisfaction of the
requirements for the degree of

BACHELOR OF SCIENCE

in

PHYSICS

by

Brian Colby

June 2008

The thesis of Brian Colby is approved by:

Professor Hartmut F.-W. Sadrozinski
Technical Advisor

Professor David P. Belanger
Thesis Advisor

Professor David P. Belanger
Chair, Department of Physics

Abstract

Characterization of Irradiated Silicon Sensors: With Time over Threshold, Count Rate, and Cluster Size

by

Brian Colby

New methods of analyzing the data output of the upgraded Embedded Particle Tracking Silicon Microscope to better understand the properties of irradiated silicon strip detectors are described and documented. Specifically new methods of analyzing the overall count rate of silicon events in irradiated detectors, as well as breaking down count rates by individual strip. Also included are detailed analysis of Time over Threshold measurements as a new way to measure charge collected. The use of count rates to detect depletion and breakdown, and the use of cluster size to identify type inversion.

Contents

List of Figures

Acknowledgments

I would like to thank many people, my parents for talking about science and engineering at the dinner table almost every night as far back as I can remember, as well as inspiring me to succeed. I would like to thank Hartmut F.W- Sadrozinski for giving me a chance to work for him. To my lab mates, especially Chris Meyer for all his help creating a user friendly analysis suite, and to my mentor for all things digital Kunal Arya.

1 Introduction

In the ATLAS lab at the Santa Cruz Institute of Particle Physics (SCIPP), located on campus at the University of California at Santa Cruz, work is being done to characterize and understand the damage caused to silicon strip detectors (SSD's), in an attempt to determine detector properties which provide greater radiation hardness. This work is inspired by the planned luminosity upgrade for the Large Hadron Collider (LHC) [1], at the European Organization for Nuclear Research (CERN), which will expose the SSD barrel tracker in the ATLAS (A Toroidal LHC ApparatuS) experiment to much higher levels of radiation than it was originally designed for.

This project is part of SCIPP's collaboration with the international research group RD50 [2], and the ATLAS upgrade,it focuses mainly on compairing different characterization measurements taken on types of detector before and after irradiation. The work done in the ATLAS lab at SCIPP is mostly the direct measurement of diffrent properties of irradiated silicon, i.e. electrical capacitance versus voltage, current verses voltage, and the charge collection efficiency of both irradiated and un-irradiated detectors. All three of these different types of measurements are described in this thesis, with a focus on charge collection efficiency and other measurements derived from that set up.

The new work covered in this thesis are new analysis techniques based on the digital continuous readout system used, the Embedded Particle Tracking Silicon Microscope (EPTSM) [3]. It includes new uses for Time over Threshold (ToT) measurements to measure collected charge, the bulk silicon count rates to measure efficiency as well as to identify breakdown, and cluster size to find the point of type inversion.

2 Background

2.1 The ATLAS Luminosity Upgrade

The current plans for the upgrade of the LHC at CERN to the sLHC, calls for an increase in luminosity to $10^{35} cm^{-2} s^{-1}$ [1]. This increase in energy will allow the experiments running at the sLHC to extend the discovery mass scale by up to 30%. Increased levels of radiation pose a challenge to developing new silicon strip detectors to complement the upgrade. New detectors will need to be made to perform after being exposed to neutron equivalent fluences of up to 1×10^{14}. To build silicon strip detectors to be more radiation hard, efficient and accurate methods must be developed to characterize candidate designs.

2.2 History and PTSM

The original Particle Tracking Silicon Microscope (PTSM) [4], was an attempt to create an imaging device for the life sciences, using silicon strip detectors, with accurate measurements of location and intensity of radiation. The idea was to put a biological specimen on top of a SSD, then use a source of ionizing radiation and a scintillation trigger to create a density map, and thereby reconstruct an image of the target, and to help study radiation sensitivity of individual cells.

While funding for the project eventually ran out the Field Programable Gate Array (FPGA) code and set up, created for PTSM, could be easily adapted to the characterization of silicon strip detectors.

2.3 Embedded Particle Tracking Silicon Microscope

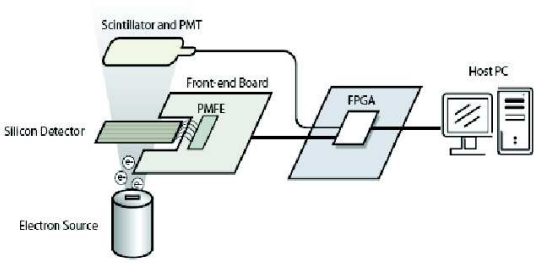

Figure 2.1: Digram of charge collection efficiency measurement test set up, including EPTSM

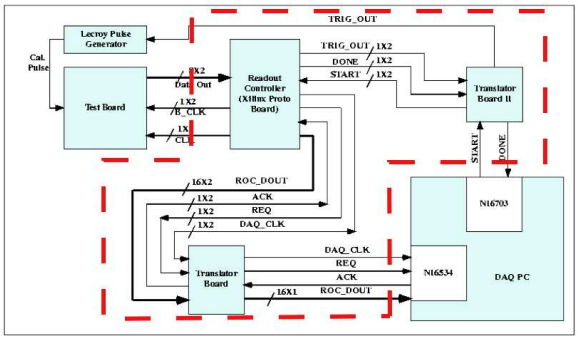

Figure 2.2: Block diagram for the original PTSM set up, the area marked by hashed lines indicate the section replaced with an FPGA.

The Embedded Particle Tracking Silicon Microscope, (EPTSM) [3], is the successor to the original Particle Tracking Silicon Microscope. It is a device designed to read out 64 channels from a silicon strip detector, as well as a trigger from a scintillator, affix timing information and then output all the data to a computer over an Ethernet connection in to an indexed ROOT file.

Previously, on the original system, several translator boards were required to both receive control signals from the operating computer, as well as return data to the computer. The old system was also rather temperamental and fragile. By switching to an embedded system, with a CPU and network driver, the system was made more user friendly and robust.

Unlike similar set ups used to measure the charge collection efficiency of silicon strip detectors, EPTSM is designed on a free running (self-triggered) read out model. That is to say, that every event in the silicon or the scintillator which is above the threshold gets recorded; instead of only recording silicon events when the scintillator counter has been triggered. Because of this, EPTSM had to be capable of the simultaneous read out of all 64 channels and the scintillator on every clock cycle, and required a large enough buffer to hold many events on the FPGA before being able to pipe the information along to the controlling computer [3].

An event does not simply occur during a single clockcycle though, to retain a measurement

of the charge deposited on a given strip EPTSM records the length of time the channel spends above threshold (ToT). To achieve this goal, EPTSM actually measures positive and negative threshold crossings. When the voltage read off a strip, through a shaper and amplifier, becomes higher than the set threshold a positive crossing is recorded by EPTSM. Likewise when the signal drops below the threshold a negative crossing is recorded. By comparing the timestamps of these two signals, the ToT can be calculated and stored along with the rest of the information on the host computer.

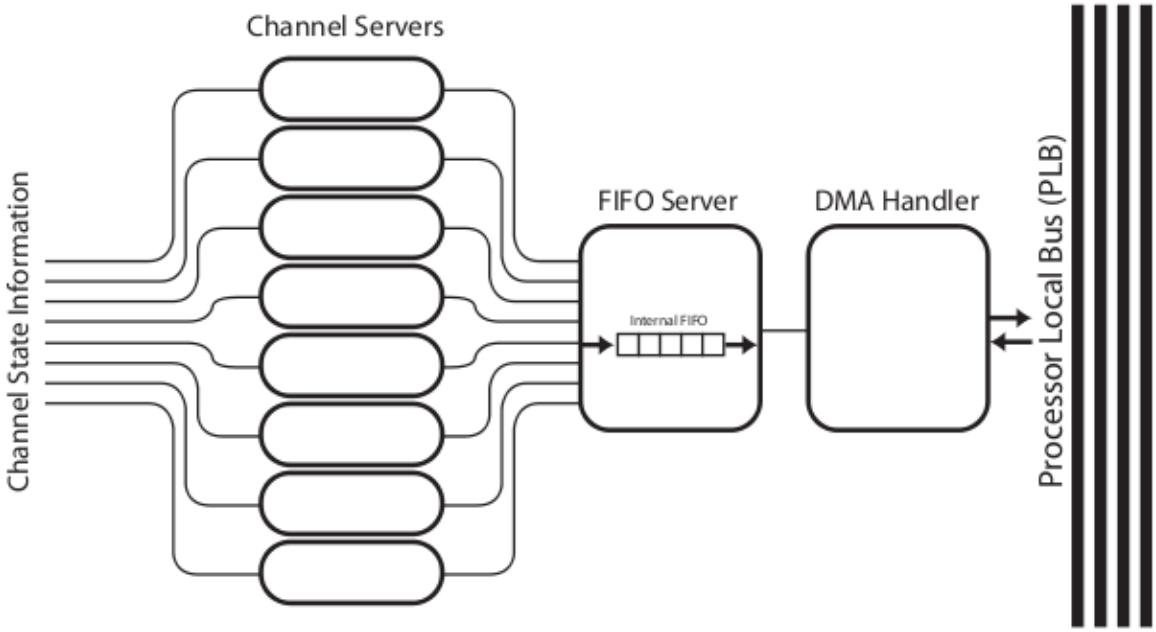

Figure 2.3: Diagram outlining the architecture of the EPTSM channel servers and FIFO. Data is read out of the PMFE in parallel by each of the channel servers, and is then serialized for output to the operating computer through the FIFO, which also acts as a buffer between the read out, and final storage on the operating computer.

To accomplish this simultaneous, and high volume read out system, a set of 16 "channel servers" were included in the design. Each channel server contained a first in first out, (FIFO), memory buffer and is hard wired to 4 channels. Then information is transferred inside the FPGA to the large channel server, with a much larger memory buffer, and control logic to take data from individual channel servers on a first come first server basis in an attempt to maintain the time

continuity of the events. If one of the individual channel servers were to become overloaded with events, such as in the case of a "hot channel" the large channel server is capable of transferring the entire content of the overloaded channel server all at once.

After being moved in parallel from the Particle Microscope Front End chip (PMFE) to the channel servers to the "Big FIFO" on the EPTSM board, data is serialized in preparation to be transferred to a computer over an Ethernet connection. These transactions are handled by a Xilinx proprietary FPGA network driver called Light Weight IP (LWIP). Using Ethernet instead of a translator board to get data off EPTSM made having an embedded system with a CPU and main bus truly critical.

2.4 The Detector Board

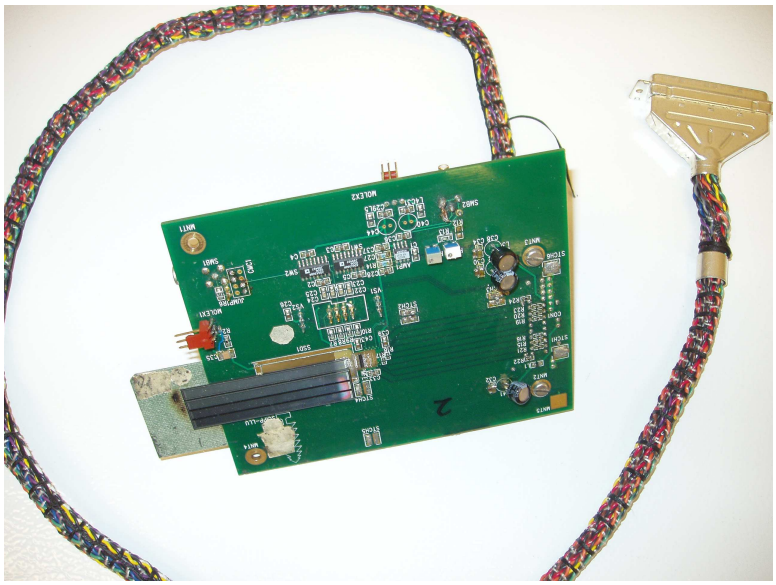

Figure 2.4: Picture of the original PTSM detector board, with silicon strip detector mounted and bonded to PMFE. These older boards had cabling soldered directly to output pins on the board, as well as several other simple design problems.

Another critical component of EPTSM is the detector board. A printed circuit board designed to hold both a silicon strip detector, and the read out ASIC, PMFE, [4] to compare

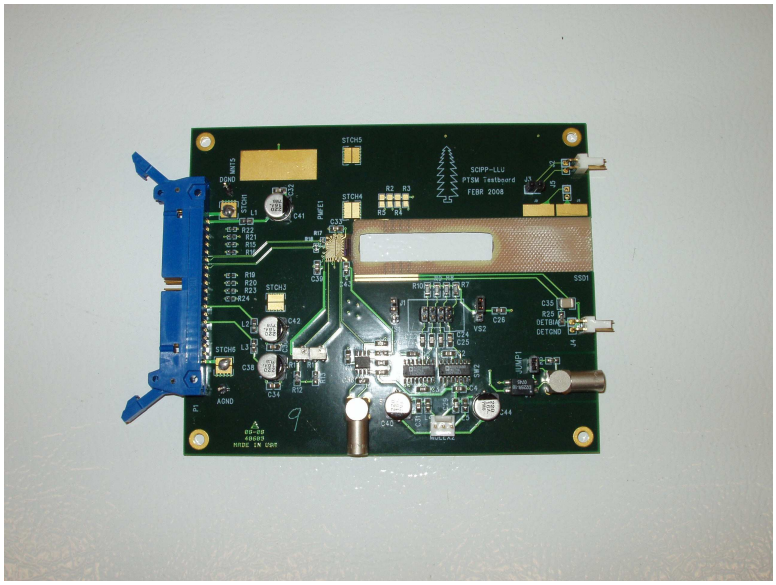

Figure 2.5: The upgraded EPTSM detector board, added in a connector for output cabling, vastly reducing complexity. Also major improvements made in noise levels by isolating analog and digital ground planes.

charges deposited on the strips of a silicon detector to an applied threshold, and send digital signals which can be interpreted by EPTSM. The board is also used to rout an externally applied bias voltage from a power supply to the bias ring of the detector. As well as routing input from a pulser to the calibration buses on the PMFE chip, and holding a thermistor to measure the operating temperature of the detector.

For testing, an irradiated silicon strip detector is secured to the opening milled out of the board with a small amount of conductive epoxy, then each of the 64 available inputs on the PMFE are bonded to 64 of the channels on the detector. If the pitch of the detector is significantly wider than the pitch of the PMFE channel input pads, a pitch adapter is utilized. Recently the detector boards underwent an overhaul, and the layout was redesigned. The second version of the detector board features many advantages, including better management of ground planes for reduced noise, and several cable management improvements.

3 Detector Characterization

3.1 Capacitance vs Voltage

One of the simplest methods of characterizing silicon strip detectors is to take a capacitance verses voltage, or CV, measurement. The capacitance of a silicon strip detector is a good indicator of the size of the depleted region. As the bias voltage applied to the detector causes an electric field inside of the detector, charge carriers move away from the junction forming a depleted region. A diagram showing the approximation of a silicon strip detector as a parallel plate capacitor due to its depleted region 3.1 exemplifies the utility of the CV measurement.

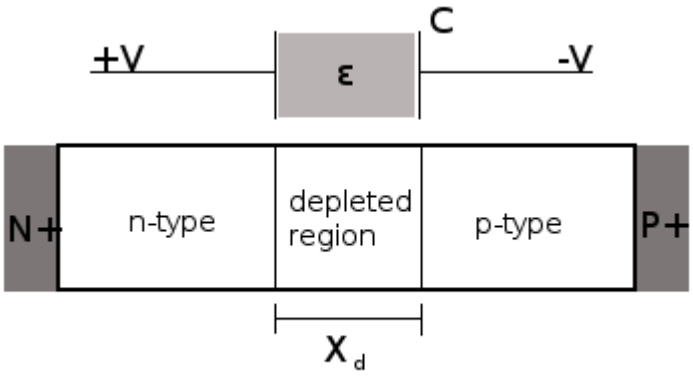

Figure 3.1: The depleted region of a P-N junction can be modeled as a parallel plate capacitor with a dielectric between the plates

Using the simple model of a parallel plate capacitor with a dielectric between the plates, it is easy to see how a larger capacitance corresponds to a smaller separation between the plates,

similar to the width of the depleted region. Capacitance for a parallel plate capacitor can also be described by the area of the plates A, the dielectric constant of the material between the plates ϵ, and the separation between the plates X_d.

$$X_d = \frac{\epsilon A}{C}$$

Solving for the width of the depleted region, it is seen that the the width of the depleted region of the P-N junction is directly related to the voltage, and inversely related to the capacitance.

3.2 Current vs Voltage

IV measurements are measurements of the leakage current through the detector when verses the bias voltage applied. The measurement of current verses voltage (IV) is critical to understanding the properties of both irradiated and un-irradiated detectors. Measurements of IV can be used to determine breakdown voltages, depletion voltage, the levels of fluence the detector has been exposed to, as well as if the detector has begun to malefunction.

3.3 Charge Collection Efficiency

The EPTSM system is used primarily for the measurement of detector Charge Collection Efficiency (CCE). The Charge collection efficiency is a measurement of the fraction of charge collected by a detector to charge passing through a detector, and is measured for irradiated detectors across a range of bias voltages and thresholds. By using a scintillation counter as a "trigger," the number of charged particles that actually passed through a detector can be measured and can be compared to the simultanious hits in the detector. The amount of collected charge can be approximated based on depletion length.

$$Q_{collected} \approx X_d + \frac{80e^-}{cm}$$

The output from the scintillator used with EPTSM is fed through a rack mounted discriminator to allow a threshold to be set, only allowing detections of particles with a minimum energy to be

counted. After passing through a discriminator, the signal is fed into a TTL gate generator, which sends a digital signal to EPTSM, where it is converted into a LVDS regime. The board treats this trigger input as another "channel" and records the scintillation trigger in the data stream as channel zero.

Because there is a non negligible propagation time between scintillation and EPTSM's registration of the trigger, the FPGA records the time stamp for channel zero events with an offset, which can be measured and set into the control software. In the set up used in our lab, this offset is set to 3 clock cycles, or 300 nanoseconds.

After a complete data set is taken for a detector, with several different thresholds and bias voltages, all of the raw output data files are run through the analysis package, one component of which measures CCE. This is done by scrubbing through the data output looking for channel zero events, which correspond to scintillations. Once a trigger is identified, the code searches for coincidences, which are silicon events on any of the 64 channels which occurred within a certain window of time around the trigger event. This time window is used to take into account variables effecting the time between a charged particle passing through the detector and being picked up by the scintillator, as well as the delay caused by the parallel-to-serial conversion.

Once the entire data file has been scanned for coincidences, the efficiency is measured by comparing the number of coincidences to the number of triggers. A one hundred percent efficient detector is one which has a hit on a channel corresponding to each hit on the scintillating trigger.

4 Computer based analysis

4.1 ROOT

ROOT is a collection of libraries and classes for C++ designed by particle physicists at CERN to organize, plot, and analyze large amounts of data. EPTSM was designed for the serial output to be sent to a computer, where the data is complied in the ROOT format. ROOT files are compressed data files organized by a "tree", with each event being a "branch" and each piece of data recorded for a given event: channel, start time, time over threshold, excreta, being a "leaf." This indexed data format is extremely useful when creating analysis software to parse the large data sets output by EPTSM.

Other useful features of the ROOT libraries are the plotting and graphics features. ROOT makes it simple to create plots, and histograms, display them on the screen, and save the displayed output as an image, without having to work through an intermediary plotting program.

ROOT was a good choice for this project, not only because of its useful tools for dealing with large data sets, ROOT is also very portable. Because it is just a collection of C++ libraries and header files, ROOT can be employed in a program which can be utilized on any platform with a C++ compiler.

4.2 Analysis-Share

The original method of converting the large amounts of raw data output from EPTSM into a manageable and human readable form was a program called Analysis Share, written by Brian Keeney. Analysis Share had to be run on each individual output file, for every threshold step at every bias voltage, and was very time consuming.

Analysis Share simply stepped through the indexed root file searching for trigger events. After locating a scintillation trigger event, hooked into the PTSM channel 0, Analysis Share would then look forward and backward a certain number of entries in the root file, attempting to locate a silicon event with a start time within a small window of time around the start time of the scintillation trigger.

With the exception of the large amount of human labor required to run the analysis of a data set with this method, Analysis Share did a fine job of collecting the relevant information out of the PTSM output files. Unfortunately it was written with a very specific goal in mind, it performed a few simple jobs, and on the whole was designed with no room for expansion. The program was limited to calculating gains from calibration data, the efficiency of a measurement, and then combining those two pieces of information to find the median charge collected.

During the early parts of my expansion of the analysis suit used in conjunction with PTSM, Analysis Share played a vital role by exporting the compressed root files into legible textual output. Being able to actually see the lines of data proved invaluable for coming to an understanding of the data structure, and later the design and debugging of new analysis scripts. Also the shear tedium of running the program helped facilitate the collaboration between Chris Meyer and myself to create a modular, expandable, automated analysis package.

4.3 Updated Computer Analysis

In conjunction with co worker Chris Meyer, many improvements to the computer based analysis have been made. To bring the analysis code abreast with the newly updated EPTSM, Chris set out to create an automated framework for performing analysis of data from EPTSM. In doing so he made the new analysis suit modular and expandable, so that new routines could be easily added and made to utilize the over all automation.

4.4 Count Rate

One of the clearest indicators of data quality is a plot of count rates, including silicon events which do not coincide with a scintillation trigger. By taking all of the silicon activity into account, regardless of whether there was a congruent trigger signal or not, it becomes obvious when detectors begin to break down. As bias voltage is increased the count rate tends to increase steadily early on, and level out around full depletion. After full depletion the count rate tends to continue being constant. If a detector reaches breakdown after being fully depleted it becomes obvious from the count rate, as the rate suddenly spikes, indicating the onset of breakdown. This behavior can be clearly seen in Figure 4.1. The sudden spike after 1000 Volts, following an almost constant count rate is indicative of breakdown in the detector.

In Figure 4.2, the detector does not reach full depletion by 900 Volts, but it also does not undergo dramatic break down. To take an accurate count rate measurement on the detector, the analysis suite goes through each data file, and counts the number of entries in each data file. Along the way, it excludes each entry for scintillation triggers to not skew the total number of silicon events. Also as it scans, it records the earliest start time, and the latest start time.

$$\text{Count Rate [MHz]} = 10 \times \frac{\text{Total Number of Events}}{\text{Largest Time [ns]} - \text{Smallest Time [ns]}}$$

Once a count rate in MHz has been determend for each threshold at each bias voltage, the analysis suit creates a graph, of the average count rate in the detector, at each bias voltage, for

each diffrent threshold measured. This makes it easy to use the average count rate measurement to quickly check the quality of different data points.

The measurement of counting rate is useful to track the depletion lengths of detectors because of low noise rates. Detector efficiency is well indicated by the counting rate, as can bee seen in Section 4.8. In addition, count rate is a very intuitive measure of the breakdown, at which point efficiency measurements lose validity.

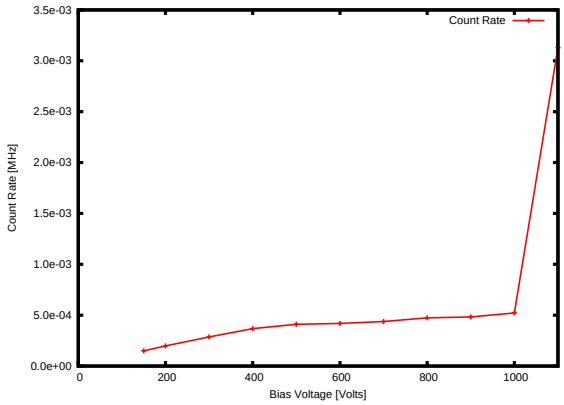

Figure 4.1: Plot of average count rate verses bias voltage. This detector, 2553-11-11, is a Micron FZ n-on-n detector, which underwent micro discharge breakdown at 1100 Volts. It was irradiated to a neutron equivalent fluence of 1×10^{15} with neutrons.

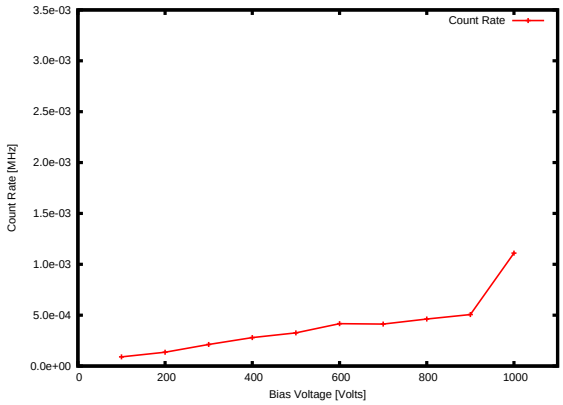

Figure 4.2: Plot of average count rate verses bias voltage. This detector, 2552-7-11, is a Micron MCz n-on-p detector, which did not undergo micro discharge breakdown. It was irradiated to a neutron equivalent fluence of 1×10^{15} with neutrons.

4.5 Count Rate by Strip

Breaking down the count rate measurement by each individual strip, can be very useful. By looking at the count rate on each individual strip, it can be determined whether or not sudden increases in over all count rate are caused by increases in activity across the entire detector, or simply a single channel going hot, or breaking down. Another useful feature of extracting the count rate on a strip by strip basis, is that when a plot is made for each bias voltage individually, the beam profile shows up clearly before and after full depletion.

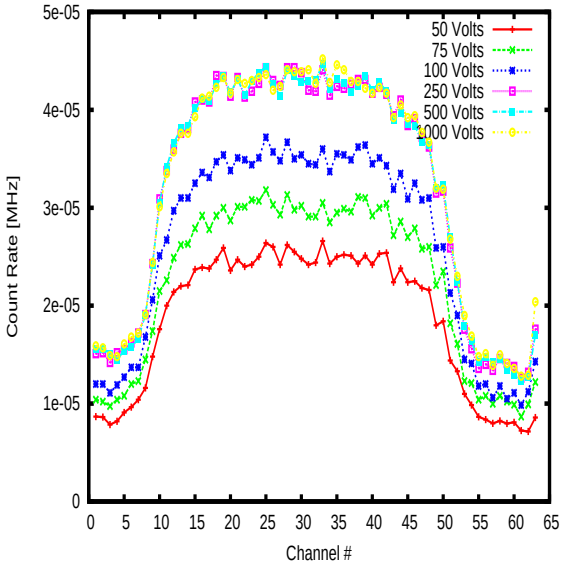

Figure 4.3: Plot of the average count rate for each strip for several different bias voltages. After the detector reaches depletion around 150 Volts, count rate becomes relatively independent of bias voltage. Also the beam profile can be clearly seen at all bias voltages, with the channels towards the center of the detector seeing a $2 \times 10^{-5} MHz$ increase in count rate.

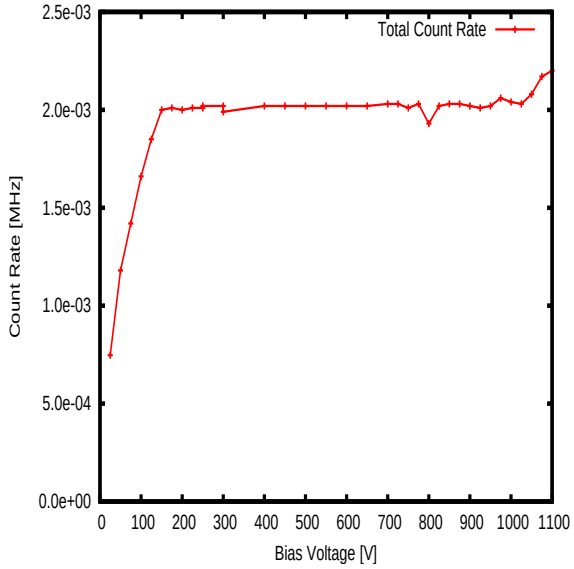

Figure 4.4: A plot of the total count rate in MHz verses bias voltage for the same data as pictured to the left in Figure 4.5. The detector reaches depletion around 150 Volts, after which the total count rate remains almost constant.

4.6 Cluster Size

By observing the number of strips which pick up charge within the time window surrounding a hit on the scintillation trigger, space charge sign inversion can be observed in irradiated detectors. For N on N Fz detectors before irradiation, there is a diode junction between the P type backplane and the N type bulk as seen in Figure 4.6. During heavy irradiation the N type bulk in these detectors undergoes type inversion and switches to a P type bulk diagrammed in Figure 4.6. When testing these N on N detectors a negative bias voltage is applied to the P type backplane, to attract electrons to the strips.

As the bias voltage applied to the detectors is increased the detector begins to deplete from the diode junction. In the case of these N on N detectors, before irradiation there is a large distance

from the beginning of the depletion region to the strips. Charge deposited in this depletion region induces charge on many strips, giving the detector a chance to pick up charge on more than one strip, leading to large clusters.

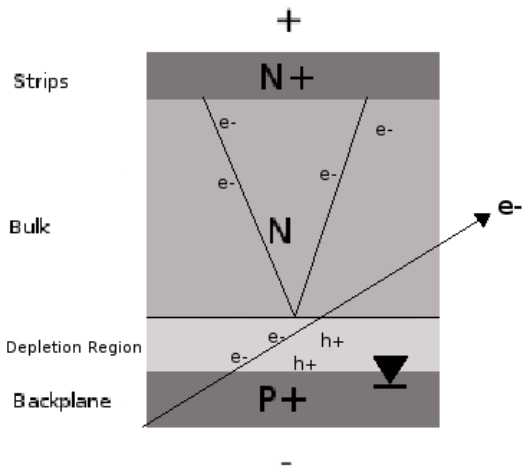

Figure 4.5: Diagram of an N on N detector before type inversion depicting deposition of charge in the depleted region. The detector depletes from the diode junction, which is between the P+ back plane and the N type bulk. Ionizing radiation deposits charge in the depleted region and has time to diffuse while traveling through the un-depleted bulk, depositing charge on more than one strip.

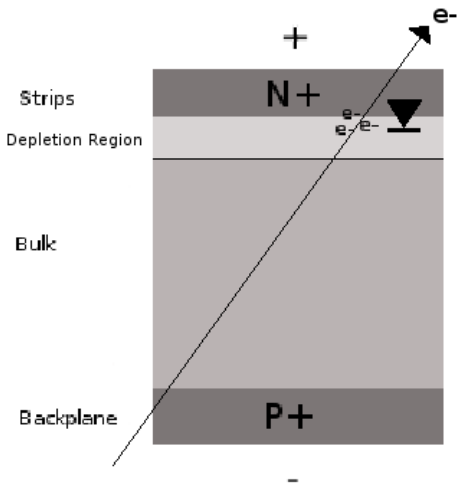

Figure 4.6: Diagram of an N on N detector after type inversion. The N type bulk has undergone space charge sign inversion, and is now effectively P type, moving the diode junction from the backplane to the strips. The reduced distance between the depleted region and the strips reduces the amount of diffusion which takes place after charge is deposited, reducing clusters.

Before irradiation causing type inversion in the N type bulk, N on N detectors perform rather poorly. But after being exposed to irradiation they perform quite well. Figure 4.6 is a histogram of cluster size for detector 2553-11-11, a N on N MCz detector irradiated to 1×10^{15} with neutrons. This detector underwent type inversion due to the irradiation, as can be seen by the low ratio of cluster sizes greater than one.

The opposite problem is run into with the irradiation of P on N Fz detectors (Figures 4.6 and 4.6). After being exposed to high amounts of radiation, the N type bulk can invert, becoming P type. This inversion moves the diode junction from just below the strips to the N type back plane, as illustrated in Figure 4.6. This inversion moves the depletion region to the back of the detector,

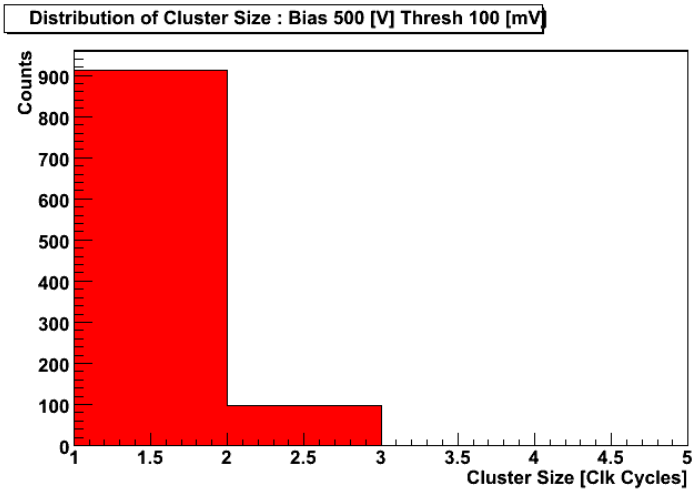

Figure 4.7: Distribution of cluster size for 2553-11-11, an N on N MCz detector, which underwent type inversion after being exposed to a fluence of 1×10^{15} with neutrons. The ratio of cluster sizes greater than one is small, at about 11%, indicating type inversion as diagrammed in Figure 4.6.

increasing the distance over which deposited charge will diffuse, leading to extra clusters. Also note the difference in bias voltage polarity required for P on N detectors.

After large amounts of radiation, P on N detectors become quite problematic due to type inversion. As can be seen in Figure 4.6, detector 2535-8-3-1, a P on N FZ device, exhibited a large number of clusters after being exposed to a neutron equivalent fluence of 2.98×10^{14} with protons. This is indicative of the type inversion behavior outlined by Figure 4.6.

Calculating the ratio of clustered events to single events is very useful for understanding the way radiation effects silicon strip detectors. By looking at this ratio for detectors with the same architecture across many diffrent fluence steps, one would be able to identify the level of radiation at which the N type bulk undergoes inversion. It should also be very interesting to compare cluster behavior for detectors across many annealing steps.

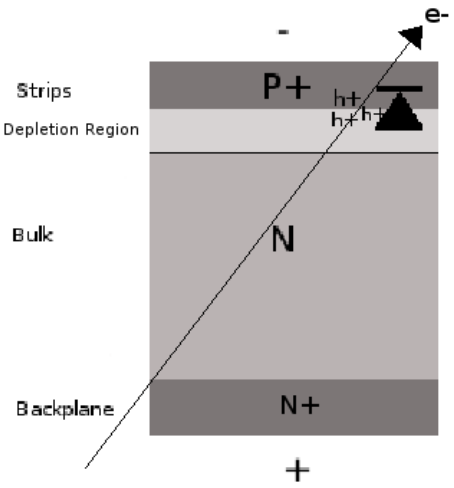

Figure 4.8: Diagram of an P on N detector before type inversion. Biased with a positive voltage on the back plane, causing holes to move to the P type strips. The depletion region begins at the diode junction between the N type bulk material and the P type strip implants, leaving little time for deposited charge to diffuse before reaching the strips.

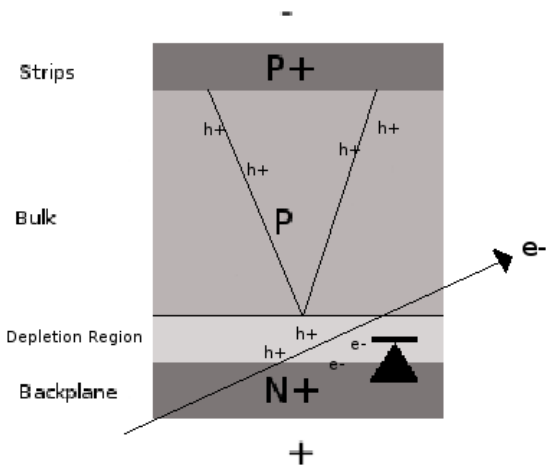

Figure 4.9: Diagram of an P on N detector after type inversion. The N type bulk has undergone space charge sign inversion, moving the diode junction to the N type backplane. Now the depletion region has moved to the back of the detector, allowing charges deposited by ionizing radiation to diffuse leading to clusters.

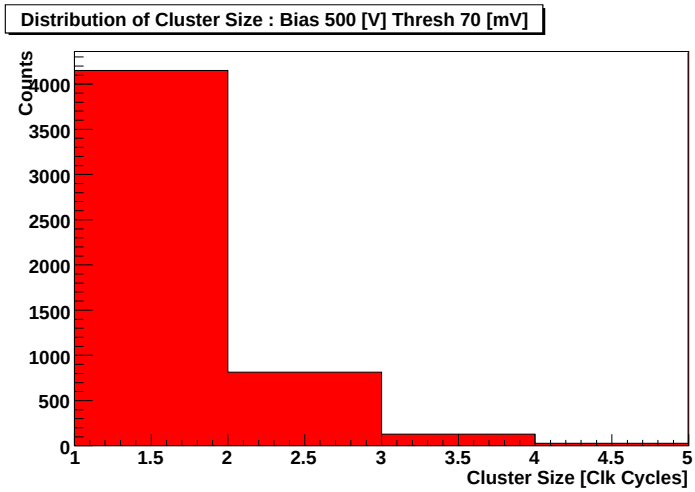

Figure 4.10: Distribution of cluster size for 2535-8-3-1, a P on N FZ detector, which underwent type inversion after being exposed to a neutron equivalent fluence of 2.98×10^{14} with protons. The ratio of cluster sizes greater than one is large, at about 25%, implying the long distance between the depletion region and the P N junction as diagrammed in Figure 4.6.

4.7 ToT

One of the most important outputs of the EPTSM system is the Time over Threshold, or ToT, recorded for each event. ToT is the difference between the time of a given signal's positive threshold crossing and the same signal's negative threshold crossing. TOT is interesting because it has a direct corelation to the charge picked up by a particular strip.

The actual amount of charge described by a given TOT measurement is determined by properties of the read out chip, rise time, shaping etc, and the actual threshold levels. Utilizing an external pulse generator, and the 4 calibration buses built into the PMFE, a comparison between ToT and the amount of charge deposited on a read out strip can be determined. As described in section 2.4, EPTSM is able to select one of four calibration bus inputs on the PMFE, and rout input from the external pulser to it.

EPTSM has built into its control code a mechanism to automate the calibration of the PMFE through the use of a general purpose interface bus (GPIB) controlled pulser, and a power supply to provide the threshold voltage. The control code sends commands to the pulser and to the threshold power supply to step through what ever combinations of input voltage and threshold are asked for through user input. The output from these calibration inputs are all compiled together into a single output root file.

At the front input of each channel of the PMFE, there is a $50fF$ capacitor connecting it to one of the 4 calibration buses. By applying a known voltage to this capacitor, from which the amount of charge can be calculated ($Q = VC$), a relation between time over threshold and charge deposited on a channel can be determined.

In Figure 4.11, there is a regular error in the ToT measurement which may be caused by issues in the parallel to serial conversion or by a binning error. As can be seen from the calculated value of the noise σ_{ToT}, this systematic effect is too large to be smoothed out by noise. It would be interesting to further investigate the cause of this behavior. This measurement can also be used to determine the uncertainty on a ToT measurement σ_{ToT}.

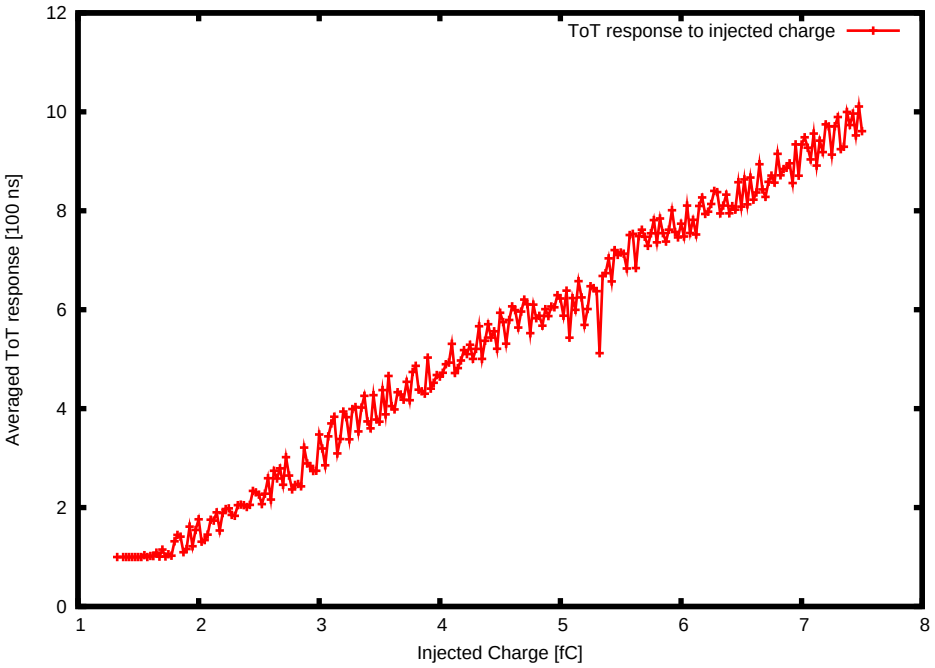

Figure 4.11: Plot of measured ToT response of the PMFE to known voltage pulses sent through a $50fC$ charging capacitor with linear fit. As can be seen from the plot, the ToT response to charge is linear.

$$\sigma_{ToT} = \frac{dToT}{dQ}\sigma_Q$$

From the slope of the fit line and the known value for the system noise of $\sigma_Q = 600e^-$ which converts to a charge of $0.95fC$, the resulting value for the standard deviation on ToT measurements is found to be

$$\sigma_{ToT} = 15[ns]$$

as seen in Figure 4.11, the relationship between ToT and the charge deposited on a strip is very linear. Using this plot one can relate time over threshold measurements taken with EPTSM to the amount of charge collected. This provides a mechanism for calculating the charge collected by a SSD in addition to the threshold curves, where the median charge is derived at the threshold setting for which the counting rate reads 50%. By calculating the median ToT for in time hits, and then comparing those values by bias voltage, to the median charge calculated, one can see very good

agreement.

A linear fit to the data presented in Figure 4.11 provides a function for ToT in terms of charge. By taking this measurement of ToT relative to input charge across several threshold voltages, a function to describe the change in ToT response with threshold voltage can be determined.

$$ToT(Q_{injected}, V_{threshold}) = a(V_{threshold}) \times Q + b(V_{threshold})$$

Where $a(V_{threshold})$ and $b(V_{threshold}$ depend upon the threshold set. Figure 4.7 shows how a varies with threshold, and Figure 4.7 shows how b vary with threshold. This function is not used in Section 4.8, to correct for the difference between the threshold used during data collection, and the true $1fC$ threshold level for the board. In the future it would be nice to perfect this method to convert ToT measurements into charge measurements to better compair ToT to median Q.

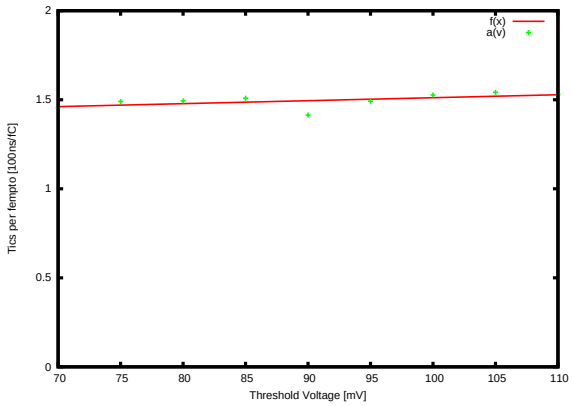

Figure 4.12: This plot displays the way the slope of the fit $ToT(Q)$ changes with threshold. It is almost constant with threshold

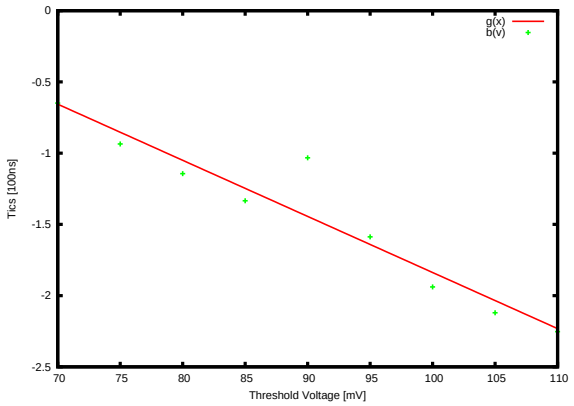

Figure 4.13: This plot displays the way the offset of the fit $ToT(Q)$ changes with threshold. It is negative and decreases linearly with threshold

4.8 Comparisons between measurements

Each of the individual measurements described above can be extremely helpful in both characterizing and understanding the damage inside of silicon strip detectors. There is even more to be learned by comparing different measurements. The close correlation between the counting rate and the efficiency has been discussed in Section 4.4, and is shown in Figures 4.14, 4.16, and 4.18.

By using the data presented in Figure 4.11, and through the method described in Section 4.7, a ToT measurement can be converted into a charge measurement. By comparing the median ToT measured in a data set to the median charge measured in that same data set, one should be able to see a correlation.

As can be seen from all three of these example detectors, the total count rate of all silicon events serves as an excellent approximation for the efficiency of a detector. This count rate measurement also is very useful for spotting the bias voltage at which breakdown occurs in a detector. This breakdown is seen clearly in all three examples, at around 700 Volts for Figure 4.14, 900 Volts for Figure 4.18, and 1000 Volts for Figure 4.16.

As can clearly be seen from Figure 4.15, after using the relationship between ToT and median charge seen in Figure 4.11, the median ToT recorded at a given bias voltage is an excellent indication of the median charge collected by the detector at that bias voltage.

While there is a noticeable and constant offset between the ToT and median charge curves in both Figure 4.15 and Figure 4.17, the offsets are opposite. With the ToT measurement being consistently lower than the median charge for 2535-8-3-1, and consistently higher than the median charge for 2553-11-11. This offset is due to the fact that the actual threshold used during the measurement of these detectors was not actually $1fC$. Median charge measurement are calculated for a $1fC$ threshold.

For N on N detectors and N on P detectors a negative threshold is required because the signals being read off the strips are negative. But for P on N detectors, this is not the case, positive signals are being read off the strips, and therefor positive thresholds are required.

For this reason the detector board was designed with the ability to switch threshold polarity between negative and positive through the use of a few jumpers which control a push down pull up system on the board, so that the voltage supplying the threshold does not need to change polarity. The end result of this set up is that the true $1fC$ for the positive polarity, the $1fC$ point is sitting around $90mV$, and for negative polarity $110mV$. Common practice in the lab is to measure at the

lowest threshold possible for a detector, and then at $100mV$ corresponding to almost $1fC$ regardless of what kind of detector you happen to be measuring. This is the case because until this point, the only way to determine median charge from EPTSM data was through calculation of response curves, a method which corrects from this offset from a $1fC$ threshold automatically. As described in Section 4.7 ToT can be converted into charge as a function of threshold, allowing an accurate comparison to median charge to be made.

As these comparisons show, both the measurement of count rate, and of ToT can be extremely useful in understanding these irradiated silicon strip detectors. By keeping and eye on the over all count rate, it can be determined when a detector reaches depletion, and when it begins to break down. By using careful calibration methods and sufficiently long measurements at each bias voltage, ToT can be used in place of the current method of determining median charge. This would be a very useful area to explore, as it could in principal reduce the amount of data required to characterize each detector significantly by reducing the number of thresholds that have to be measured.

As discussed in Section 3.1, the capacitance of a detector at a given bias voltage can be related to the length of the depletion region. The depletion depth is related to the efficiency of the detector, as covered in Section 4.6, also as shown in this section the silicon counting rate is directly related to the efficiency of a detector. As seen in Figure 4.20, compairing a plot of $\frac{1}{C^2}$ and counting rate verses bias voltage shows very similar saturation behavior.

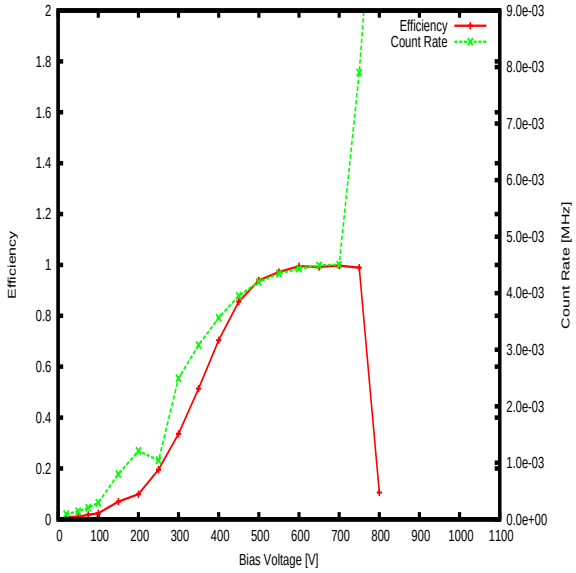

Figure 4.14: Plot of efficiency and average count rate verses bias voltage for detector 2535-8-3-1. This is a P on N FZ detector irradiated to a neutron equivalent fluence of 2.98×10^{14} with protons. This detector exhibits break down at 700 Volts.

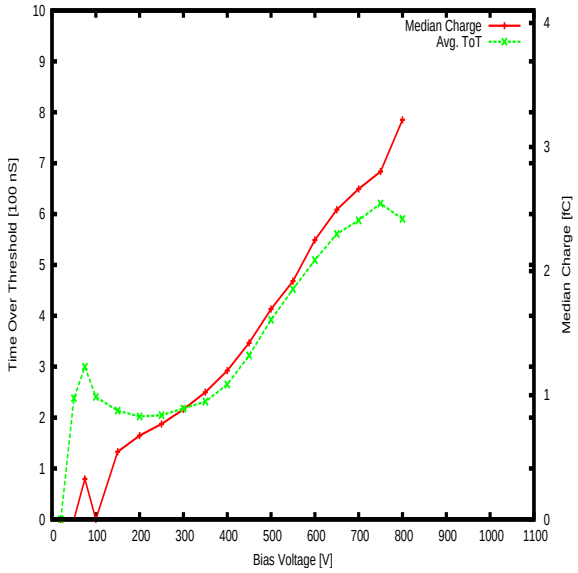

Figure 4.15: Plot of time over threshold and median charge collected verses bias voltage for detector 2535-8-3-1. The ToT measurement is a very good approximation for the median charge, because the threshold it was measured at was only slightly above $1fC$.

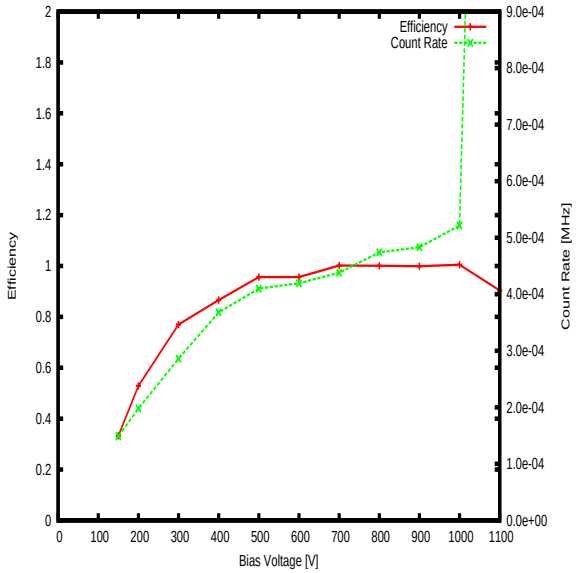

Figure 4.16: Plot of efficiency and count rate verses bias voltage for detector 2553-11-11, an N on N MCz detector irradiated to a fluence of 1×10^{15} with neutrons. This detector exhibits break down at 1000 Volts.

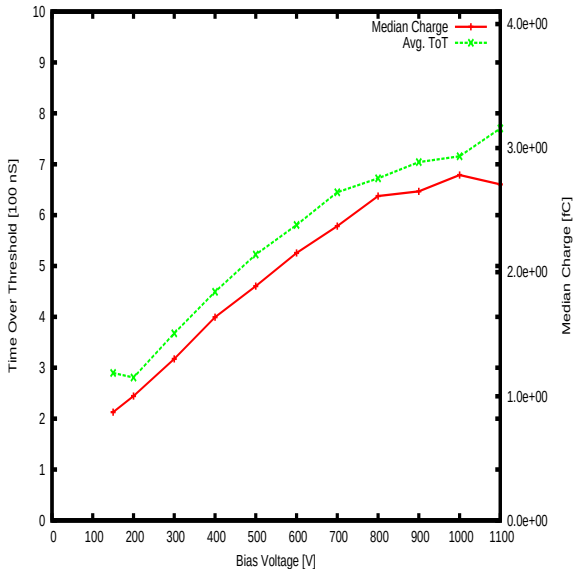

Figure 4.17: Plot of Time over Threshold and median charge collected verses bias voltage for detector 2553-11-11. The measurement for Time over Threshold is offset above the median charge measurement by a constant amount due to the threshold used during the measurement being slightly lower than $1fC$.

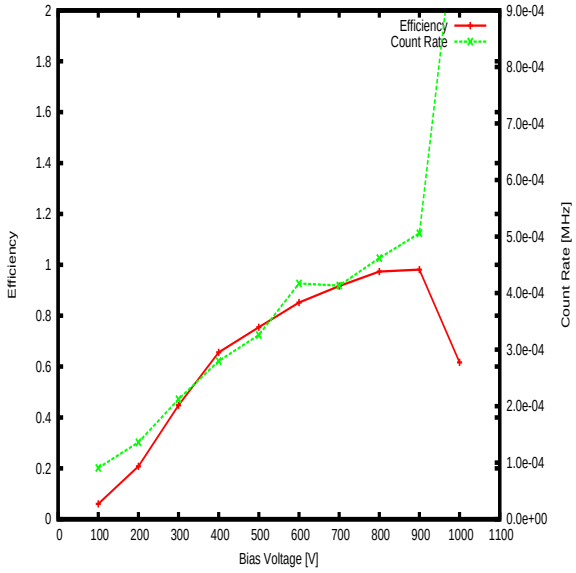

Figure 4.18: Plot of efficiency and count rate verses bias voltage for detector 2552-7-11, an N on P MCz detector irradiated to a fluence of 1×10^{15} with neutrons. This detector exhibited breakdown behavior at 900 Volts.

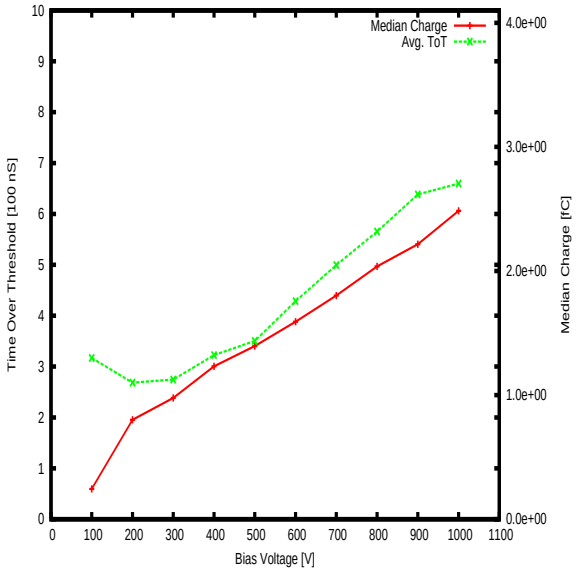

Figure 4.19: Plot of Time over Threshold and median charge collected verses bias voltage for detector 2552-7-11. The measurement of ToT is slightly above the calculated median charge due to the threshold used to measure this detector was slightly lower than $1fC$.

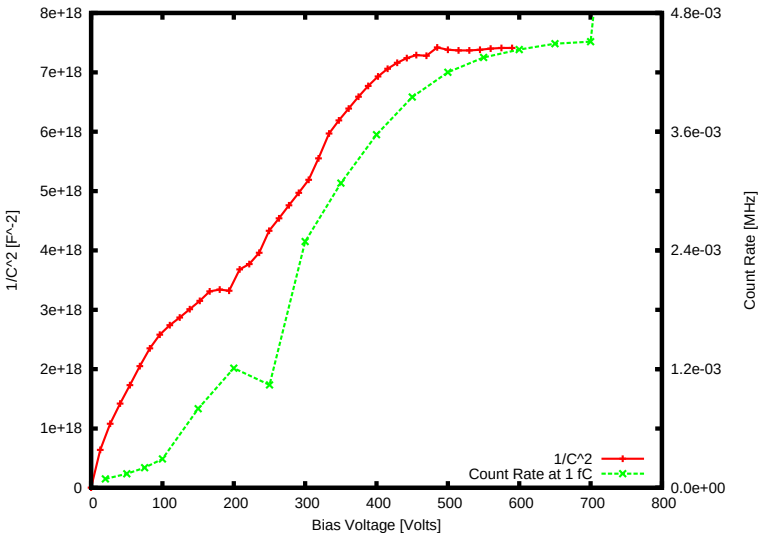

Figure 4.20: Comparison of $\frac{1}{C^2}$ verses voltage measurement and counting rate as methods of determining depletion for detector 2535-8-3-1, an N on N Fz detector irradiated to a neutron equivalent fluence of 2.98×10^{14} with protons. Both curves show similar saturation behavior in the same voltage regime.

Bibliography

[1] Hartmut F.-W. Sadrozinski, et al. “Tracking detectors for the sLHC, the LHC upgrade” SCIPP Preprint #05/14 2005

[2] RD50 research group. CERN “¡http://rd50.web.cern.ch/rd50/¿”

[3] Kunal A. Arya. “Embedded Particle Tracking Silicon Microscope: An Independent Data Aquisition System for Silicon Detector Characterization” Baskin School of Enginering UCSC 2007

[4] Brian Keeney. “The Design, Implementation, and Characterization of a Prototype Readout System for the Particle Tracking Silicon Microscope” UCSC M.S. Thesis 2004